LASER INTERFEROMETER GRAVITATIONAL WAVE OBSERVATORY
- LIGO -
CALIFORNIA INSTITUTE OF TECHNOLOGY
MASSACHUSETTS INSTITUTE OF TECHNOLOGY

Technical Note **LIGO-T010028- 00- R** 1/2/2000

Performance of STACIS seismic isolation system at the 40 Meter Lab

L. Jones, D. Ugolini, S. Vass, A. Weinstein

This is an internal working note
of the LIGO Project.

California Institute of Technology
LIGO Project - MS 18-34
Pasadena CA 91125
Phone (626) 395-2129
Fax (626) 304-9834
E-mail: info@ligo.caltech.edu

Massachusetts Institute of Technology
LIGO Project - MS NW17-161
Cambridge, MA 02139
Phone (617) 253-4824
Fax (617) 253-4824
E-mail: info@ligo.mit.edu

WWW: http://www.ligo.caltech.edu/

Performance of STACIS seismic isolation system at the 40 Meter Lab

Larry Jones, Dennis Ugolini, Steve Vass, Alan Weinstein
1/2/2000

Abstract

We describe the installation and evaluation of the STACIS seismic isolation system in the 40 Meter Laboratory test mass chambers.

1 Introduction

The Caltech 40 Meter LIGO Prototype Laboratory is being upgraded in order to prototype advanced interferometric configurations (specifically, dual recycling and DC GW readout) for Advanced LIGO. Anticipating the challenge of acquiring lock in a more complex optical configuration, we wish to reduce the effect of seismic motion (in the 1 - 100 Hz region) on lock acquisition. For the upgrade, the 40 Meter test mass mirrors will be hung from simple pendula (Initial LIGO SOS suspensions, or scaled up versions thereof), and sitting on passive seismic stacks. Seismic motion results in mirrors with significant velocity, making lock acquisition more difficult.

Seismic noise at Caltech is considerably higher than at the observatory sites, and there is much human-generated ground motion during the day. In the past, lock acquisition at the 40 meter lab has always been difficult, especially during the day. In spring 2000, we measured the ground motion at the lab, and the stack transfer functions [1]. Figure 1, taken from ref. [1], illustrates the ground noise spectrum in the wee hours.

Given the larger seismic noise at the 40m relative to the observatory sites, the extra challenge in bringing a dual recycled interferometer into lock, and the fact that Advanced LIGO will have extremely elaborate and sophisticated active seismic isolation systems, we decided to put a "poor man's" version of an active seismic isolation system under the 40m test mass chamber passive isolation stacks. After surveying the performance and availability of commercial products, we determined that only the STACIS seismic isolation system could meet our needs.

2 STACIS seismic isolation system

The STACIS seismic isolation system [2] was developed by Barry Controls, and is now manufactured by Technical Manufacturing Corp (TMC), which also makes high-quality optical tables and assorted seismic isolation products. An early version of this system was used in the MIT Phase Noise Interferometer [3]. The system consists of three independent pedestals, controlled by a single controller box. Each pedestal has a rubber sheet for passive isolation at high frequencies (pole around 12-20 Hz); and a 3-axis PZT stack to actively suppress ground motion at frequencies between 0.3 and 250 Hz. The controller supplies power to the three pedestals, and monitors the sensor and actuator levels of all three degrees of freedom (x,y,z) of all three pedestals. Serial port communications make these digitized signals available to the user's computer. A Labview-based PC program can be used to display these signals, and the overall status of each isolation pedestal.

The system is pictured in Fig. 2, with a block diagram in Fig. 3. The advertised isolation transfer functions are given in Fig. 4.

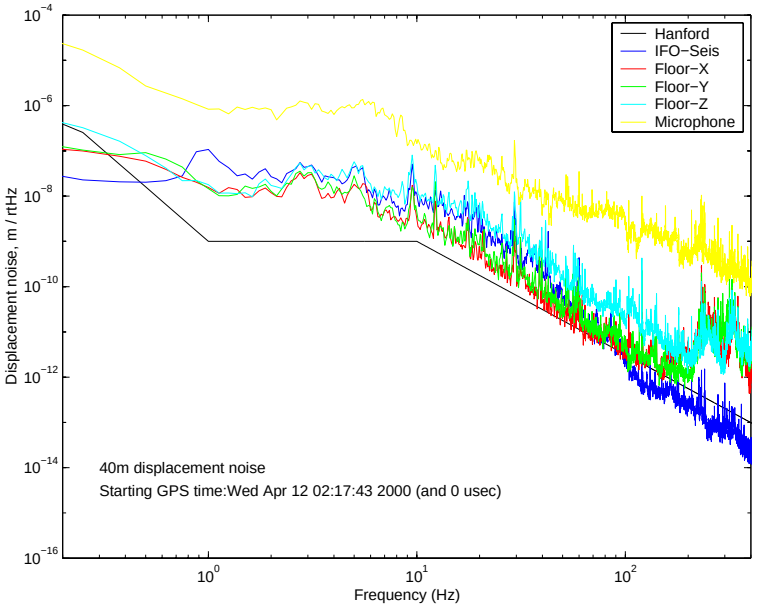

Figure 1: Ground motion at the 40m lab in Spring 2000, taken with 3-axis geophones and a seismometer, compared with the parameterized Hanford spectrum.

Figure 2: The STACIS sesimic isolation system.

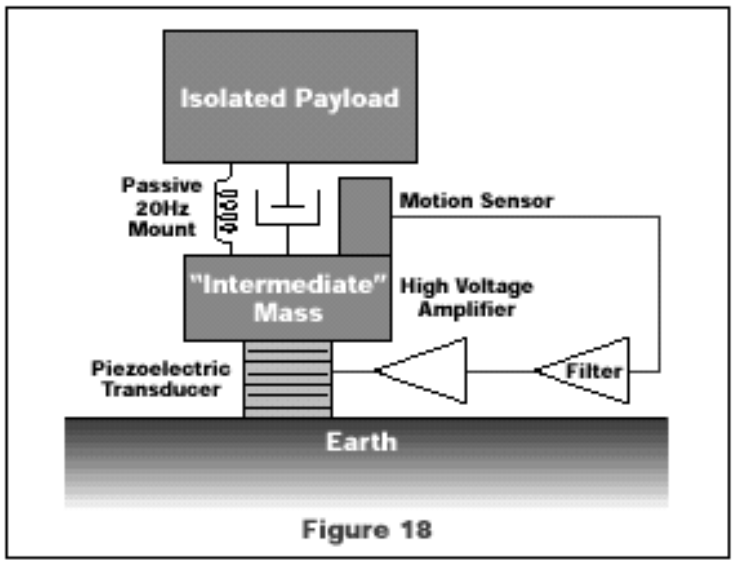

Figure 3: Block diagram of one STACIS isolation pedestal. They actually have sensors and actuators for all 3 degrees of freedom.

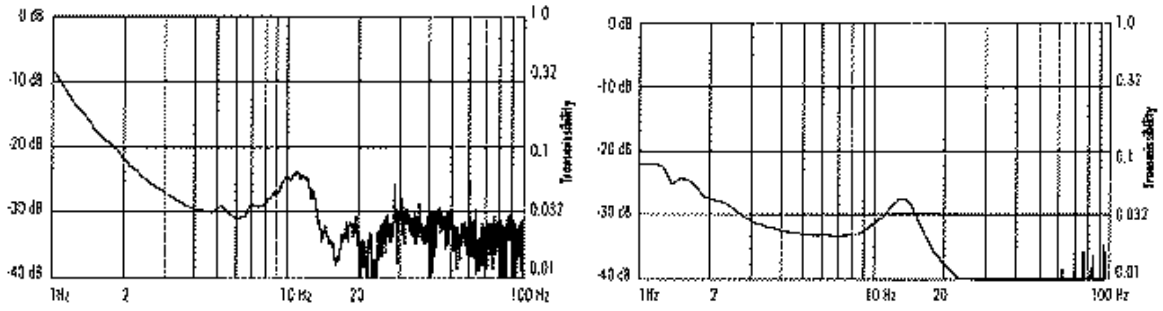

Figure 4: Advertised vertical and horizontal transmissibility.

3 Expected performance

Using a crude model of the STACIS transfer function, we can estimate the effect of the STACIS system on the mirror motion.

Of relevance is the displacement noise at high (LIGO-band) frequencies, and also the total rms velocity. The former affects our gravitational wave noise level, and the latter affects our ability to lock the interferometer. In particular, lock acquisition requires low rms velocity in the band below 100 Hz. Seismic noise peaks at the microseismic peak (around 0.2 Hz), but such low frequency motion produces little *differential* motion over 40 meter baselines; and it's differential motion that matters when locking optical cavities. We can take this into account; even still, it is not clear (to us, anyway) the degree to which motion in the $0.1 - 1.0$ Hz band adversely affects lock acquisition. Therefore, we calculate the rms velocity of the mirror by integrating down from high frequencies to 1.0 Hz, and also to 0.1 Hz. It turns out, because of the low frequency correlations, there's little contribution to the rms velocity in the $0.1 - 1.0$ Hz band, as long as the STACIS isolators do not themselve introduce significant differential motion in that band.

We measured the velocity noise spectrum at the floor, in the middle of the afternoon on 4/12/00; see the top spectrum in Fig. 5. We can model the transfer functions of the passive seismic isolation stack, and the 1.0 Hz pendulum.

We can also model the effect of the common mode motion, and residual differential mode motion across 40m [4]. The velocity of seismic waves is parameterized as:

$$v_{seis} = (450 + 1900e^{-f/2}) \text{ m/s},$$

and the correlation across a distance $d = 40$ m is

$$corr = J_0(2\pi f d / v_{seis})$$

where J_0 is the Bessel function of order 0. The net effect of this correlation on the velocity spectrum can be crudely parameterized as a unitless transfer function equal to 6×10^{-3} below 0.067 Hz; rising like $f^{1.25}$ to 1 above 4 Hz.

The effect of the passive seismic isolation stack, 1.0 Hz pendulum, and suppression of differential motion at low frequencies, is shown as the middle spectrum in Fig. 5.

Finally, we can model the STACIS transfer functions (in progress XXX). A crude model yields the bottom spectrum in Fig. 5.

The rms velocities corresponding to the spectra in the figure, are given there. We see that if the STACIS systems perform as modeled, we can expect a factor 5–10 improvement in the rms velocity at the mirror. This should have a big effect on lock acquisition, especially during the day [1], when, traditionally, the 40m interferometer lock acquisition has always been more problematical.

4 Installation of STACIS

We purchased four of these systems (at a total cost of $138K) for installation in the four test mass chambers at the 40 meter lab. The test mass chamber 3-legged seismic stacks are supported on two horizontal support beams, which exit the test mass vacuum chambers through 4 vacuum bellows. These two support beams rested on four metal feet, bolted to the floor. In November 2000, Steve Vass removed these four metal feet. These were replaced by metal brackets designed by Larry Jones and machined by Caltech CES [5] (see Fig 6). These brackets, in turn, rest on the three STACIS pedestals: two on one side of the test mass chamber, and one on the other side [6]. The STACIS pedestals rest on flat SS plates grouted to the 40m lab floor.

Between 11/27-12/6/00, Vass and Jones mounted the brackets on all four test mass chambers, and installed the STACIS pedestals under the brackets. By 12/14/00, after any/all settling, they

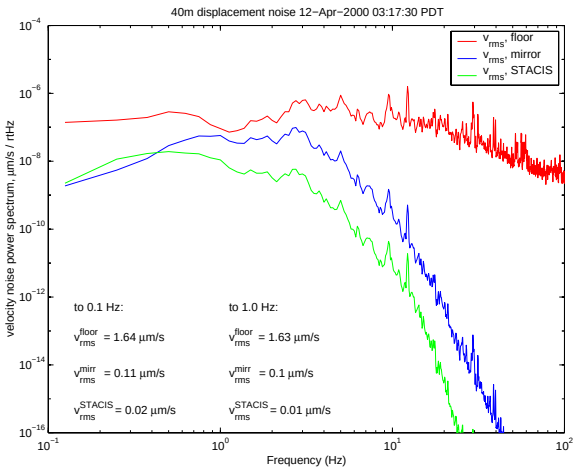

Figure 5: Velocity noise power spectra at the 40 meter. Top (red) spectrum is the velocity noise at the floor, as measured in the middle of the afternoon on 4/12/00. The middle (blue) spectrum is the same, filtered through: (a) the passive seismic isolation stack; (b) the 1.0 Hz pendulum; (c) the effect of common-mode motion at low frequencies due to seismic wavelengths on the order of 40m or longer. The bottom (green) spectrum includes also a crude model of the STACIS transfer function.

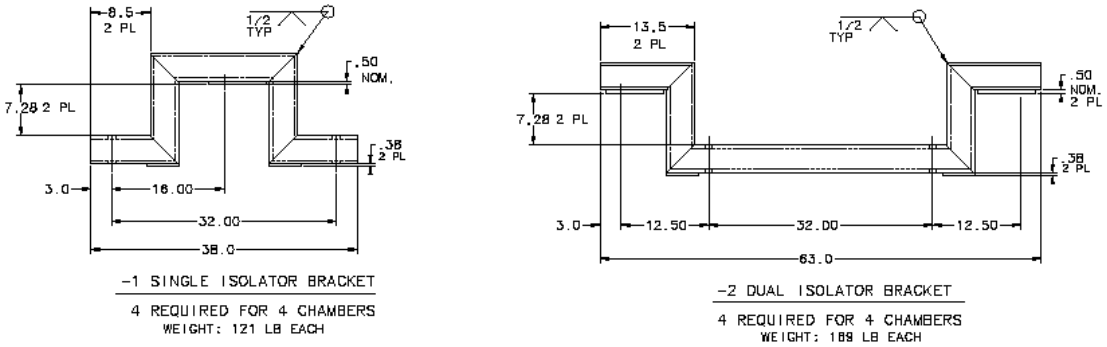

Figure 6: Brackets designed by Larry Jones to rest on one or two STACIS pedestals and support the test mass chamber stack support beams. LIGO drawing D000187.

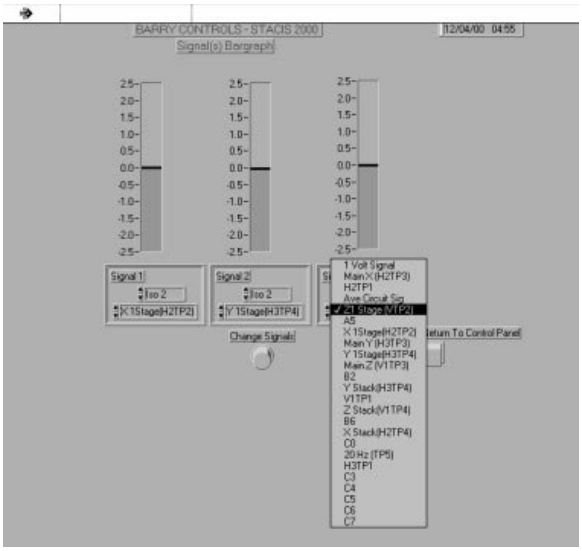

Figure 7: PC Labview-based screen showing the x,y,z control signal bargraphs for one of the isolator pedestals in the set of three.

re-measured the elevations of all the support beams, and applied shims between the support beams and brackets to esure that the support beams were level to within 0.5 mrad.

We can use a PC on a cart to look at the output of the STACIS systems, one at a time. The PC software can display bargraphs of the x,y,z control signals to the PZT actuators in each of the 3 pedestals in the system; see Fig. 7. Crude LED versions of these bargraphs are available on the controller boxes.

In order to monitor the system automatically and acquire statistics on stability and reliability of the system (as well as correlations with earthquakes), we need a VME cpu with 4 serial ports to communicate with the four STACIS controllers, as well as analog DCU hardware (AA filters and VME ADC) to continually read out a seismometer, geophones, etc. These data can then go to a DAQS system for logging as frames, or an EPICS system for logging as strip-charts, or both. (Best to have this be an EPICS crate, known as an "IOC", and then have an "EDCU" to pull the EPICS data into DAQS frames at some low rate, if desired). We plan on assembling such a system in January, 2001.

Immediately after installation of the first system, Dennis Ugolini did a bang test. He powered on the controller and watched it go through its start-up self-tests. The STACIS pedestals started humming softly. Nothing blew up! The xyz bargraphs on the controller settled into some midway position, for all three pedestals. Dennis then banged the bracket with a heavy mallet, and watched the bargraphs rail high and low (expecially the z, vertical, bargraph) for a few moments; they then settled back into the midway position. Test passed!

5 Spectra

Immediately after installation, Dennis Ugolini tested the controllers and took motion spectra with a pair of 3-axis geophones and an HP 3563A Control Systems Spectrum Analyzer in transfer function mode. The magnitude of the transfer functions in x,y,z are shown in Figs. 10 through 13. The spectra, with coherence, for each of the 12 pedestals are in Figs. 14 through 25. Various special cases are displayed in Figs. 8 and 9, and in Figs. 26 through 32.

Yes, at the moment, all the figures have mis-labeled y-axes; the transfer function is in absolute scale, not dB.

6 Discussion

6.1 STACIS turned off

The spectrum with STACIS turned off (one geophone on the floor, the other resting on the bracket which rests on the STACIS pedestal) is shown in Fig. 27.

The spectrum is flat at 1. We expected to see the effect of the passive isolator (rubber sheet) as well as all intervening material (base, bracket, etc.). The passive isolator, loaded, should give a very damped 15 Hz resonance, followed by a $1/f^2$ fall-off at higher frequencies. These features can be seen in the closed-loop transfer functions advertised on the STACIS web page, and shown in Fig. 4.

It may be that the poor coherence at large frequencies is hiding these features, or it may be that the open-loop transfer function is not as simple as we think.

The intervening material should produce resonances as low as 50 Hz. Larry Jones designed the brackets so that their lowest resonant frequency is around 50 Hz. A 57 Hz line is present (though hard to see on the log scale) in Fig. 32.

6.2 STACIS turned ON

The spectra, with coherence, for each of the 12 pedestals are in Figs. 14 through 25.

We don't see the 15 Hz passive resonance in either the OFF nor ON spectra; nor do we see the $1/f^2$ fall-off at higher frequencies (but the coherence between the two geophones is poor above 10 Hz). It's as if the pedestals are missing their rubber sheet.

6.3 Low Frequency response

Before we purchased the STACIS systems, we were warned by TMC of low-frequency motion:

> The Stacis isolators have low frequency motion at 0.1 to 0.3 hz. The amplitude varies from less than 1 um to a maximum of about 5 um (peak-peak). The motion is influenced by temperature changes and air flow over the electronics in the isolators. We have added a shield in the isolator to minimize any air movement and temperature change in the isolator, however there is still some random motion. A stable temperature and minimum air flow around the isolators at the site will minimize the motion.

This will introduce a "microseismic peak" into the 40m! We also were warned by Seiji Kawamura about a similar effect with the pneumatic isolators they use at TAMA.

So, we tried to measure the transfer functions down to 0.1 Hz (requiring 3-4 hours per run); the results are in Fig. 29.

If it wasn't for the lack of coherence below 1 Hz, this figure would be regarded as very good news! We will take more spectra to test reproducibility.

At low frequencies (< 10 Hz?), typical geophone response falls rapidly [7]. Still, transfer functions should be ok above some minimum frequency. In order to get better results at low frequencies, we need a matched pair of quality seismometers, such as the Strecheisen STS-2's used in the LIGO Tri-Net system [8] or the Advanced LIGO seismic isolation system [9]. We will try to borrow this equipment.XXX

6.4 High frequency response

It would be nice to verify the expected $1/f^2$ falloff of the transfer function due to the passive isolation, above the STACIS active bandwidth of ~100 Hz.

However, there is not much coherence in our geophone measurements below above some 10's of Hz. Why? Geophones have spurious resonances at 150 Hz. They also are prone to acoustic noise at higher frequencies (all of our measurements have been done in air). To minimize the effect of environmental vibrations (affecting the upper geophone and not the lower), we place the geophones on steel plates, and place a lead brick on top of them (it's difficult to clamp or bolt the geophones to the brackets).

Still, we find it difficult to get results with high coherence above 10's of Hz, and thus are unable to obtain clear evidence for the expected $1/f^2$ falloff.

6.5 Response from TMC

These results were brought to the attention of Pete Nelson, manager of R&D at TMC, who responded by email on 12/21/00. He said:

> I have reviewed the data you sent, and it seems to me that the system is working fine. You have missed a few important points about how STACIS functions...
>
> We modified the compensation in the STACIS servo to add a peak in the servo loop gain at the elastomeric mount resonance. This peak in the servo loop transfer function has the same frequency, height, and Q-factor as the mount. The mount still amplifies noise at its resonance, but the servo matches this amplification with increased gain.
>
> The result: your transfer functions *should not* have any evidence of a rubber mount resonance. Likewise, you should not observe a $1/f^2$ falloff in the vibration above 15Hz. It is true that the passive mount starts to provide isolation above 15Hz (though at less than a $1/f^2$ rate - rubber is funny stuff), but it is also true that the servo gain is dropping off at more or less the same rate. This results in a transfer function which is more or less flat from 15Hz up to the 100-200Hz unity gain frequency.
>
> We have made a lot of effort to reduce the drift in the STACIS system. I am glad that you don't see it. Of course, your interferometer might think otherwise. I brought this up earlier because of my experience with the GW detectors (I was a post-doc at JILA and the MPQ).
>
> CalTech has always done things on a single slab of concrete, which has forced low-frequency noise to be coherent between the endtanks. Not so with STACIS. Your end tanks will almost certainly have some level of noise which is incoherent, and should be on the order of 1 micron in amplitude. Of course, this is exactly the situation at LA and WA.

I asked Pete for a model of the transfer function for a fully-loaded STACIS, and he declined to give us one, citing "proprietory" technology and the difficulty in modeling the rubber sheet. Unfortunately, we *need* some kind of model of the STACIS response in order to model the mirror motion.

6.6 Better instrumentation

Our geophones are blue boxes (given to us by MIT). The geophones inside are unlabeled, so we don't know their specs. A calibration constant is scrawled on the box. We are not sure who made them (Barry Controls?), what their resonant frequency is, what their response in V/(m/s) is at low and high frequencies.

Typical geophone response falls off rapidly below 10 Hz, and has spurious resonances above 100 Hz. Thus, the displacement noise spectra shown in, eg, Figs. 8 and 32 are certainly wrong below 10 Hz and above 100 Hz.

We need better instrumentation! Better (well, understood) geophones; quality 3-axis seismometer pairs to measure the transfer functions down to 0.1 Hz or below; a DAQS system to write frames (rather than relying on the HP spectrum analyzer).

We await the re-assembly of our DAQ system (as early as 1/01) so that we can write the geophone and seismometer signals to frames and analyze offline.

We also need to follow up on some of the poorer spectra, and study reproducibility. We can try to take spectra on the optical table in the chamber, in vacuum. However, the motion there is so small that it may be impossible to measure with conventional instrumentation, above 10's of Hz. (That's why we need an interferometer!).

7 Summary and Conclusions

Assuming these spectra are to be believed, the STACIS isolators are providing between 20 and 30 dB of seismic isolation in the 1-100 Hz range!

This should translate into a reduction in the rms velocity of the mirrors by XXX.

We need to monitor the stability, reproducibility, and long-term reliability of the systems. We want to check their response to earthquakes.

We are now operating the STACIS systems continuously, and monitoring the 12 pedestals on a daily basis (by checking that the four controllers' xyz displays are within range for all three pdedestals). In the near future, they will be continuously monitored with EPICS.

References

[1] Measurement of Seismic Motion at 40m and transfer function of seismic stacks, D. Ugolini, S. Vass, A. Weinstein, LIGO Note T000058, 2000.

[2] http://www.techmfg.com/Products/Advanced/STACIS2000.htm

[3] Performance of the Barry Controls, Inc. STACIS Active Isolation System, Peter Fritschel and Gabriella Gonzalez, LIGO Note T950046-00-R.

[4] Thanks to Nergis Mavalvala and Gabriela Gonzalez.

[5] LIGO Drawings D000187, D000208, and D000211.

[6] For photos of STACIS pedestals installed on a 40 meter test mass chamber, see http://www.ligo.caltech.edu/~ajw/40m_stacis.html.

[7] Useful sites about geophones and their frequency response:
GEOPHONE FAQ: http://www.treefort.org/~ghost/geo.shtml
Geophone research at Stanford: http://micromachine.stanford.edu/smssl/projects/Geophones/
Geophones from i-o.com: http://www.i-o.com/htmlweb/framesetland.htm

[8] The LIGO TriNet Seismic Network Extension Project:
http://www.ligo.caltech.edu/~smarka/sne/sne.html

[9] Baseline LIGO-II Seismic Isolation Implementation Design Description, LIGO-T000024-00-U. Also: http://lsuligo.phys.lsu.edu/active/active.html

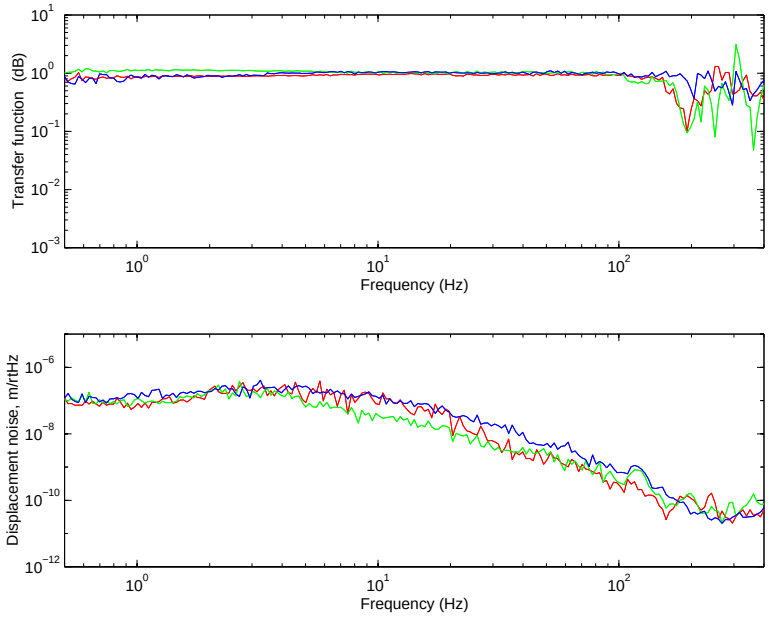

Figure 8: Top: Transfer function between the two geophones sitting side by side. Bottom: Displacement noise spectrum of the ground motion at the 40 meter lab on 11/29/00. Because of the poorly-understood frequency response of our geophones, these displacement spectra are not meaningfully calibrated, although they should have the right magnitude between 10 and 100 Hz. In both figures, red is x, green is y, and blue is z (vertical).

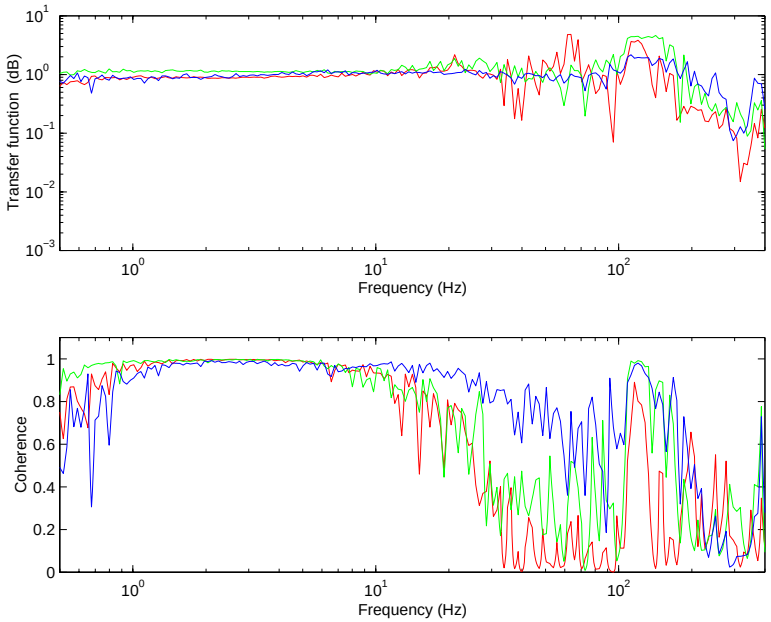

Figure 9: OFF. Top: Transfer function between the two geophones; one on the floor, the other on the top of the bracket that rests on the STACIS pedestals. The STACIS system was turned OFF. Bottom: Coherence between the two geophones. In both figures, red is x, green is y, and blue is z (vertical).

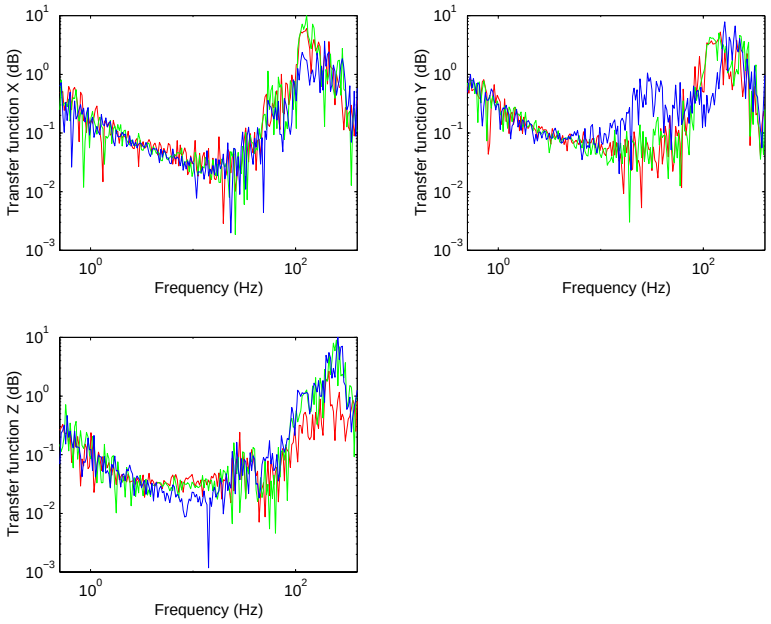

Figure 10: SE-TR. Transfer function between the two geophones; one on the floor, the other on the top of the bracket that rests on one of the three STACIS pedestals. The STACIS system was turned ON. The three figures are for X, Y, and Z (vertical). In each figure, red, green and blue traces are for the second geophone resting on each one of the three isolators in the set (red=SENE; green=SENW; blue=SES).

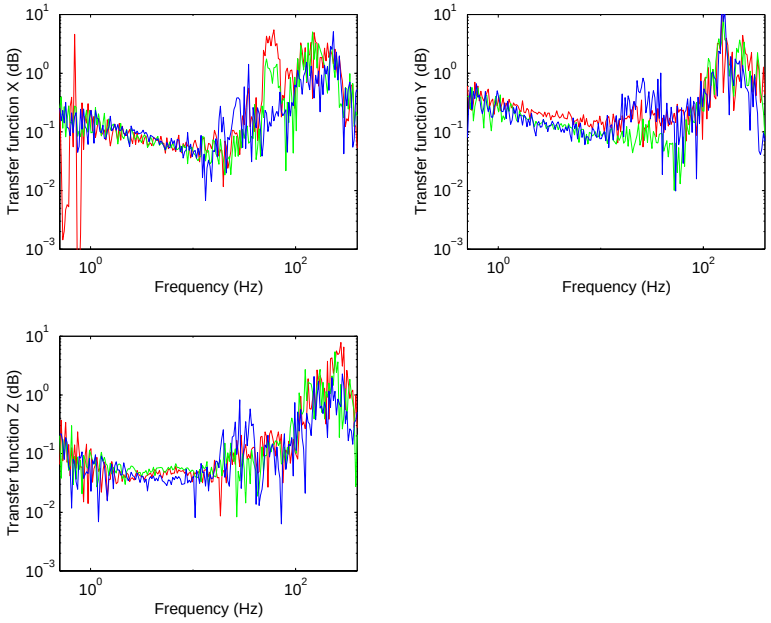

Figure 11: SV-TR. (red=SVNE; green=SVNW; blue=SVS). See caption to Fig. 10.

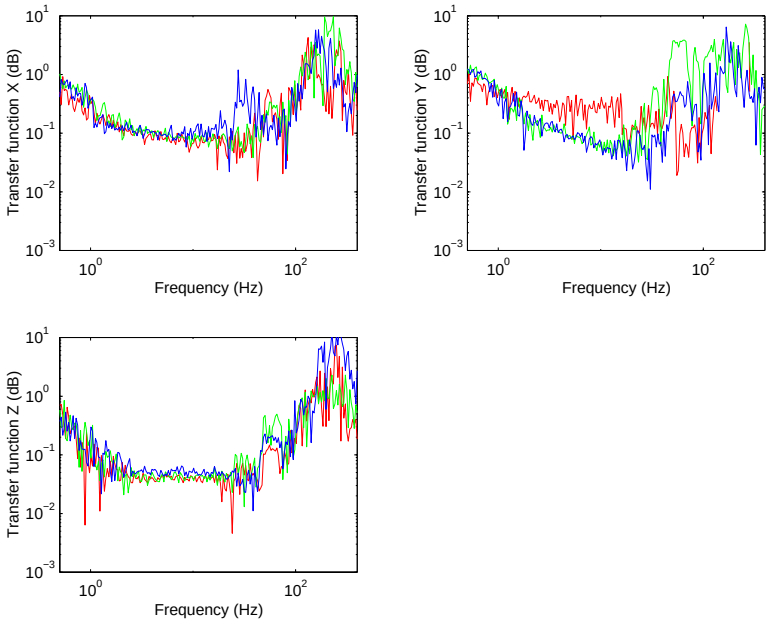

Figure 12: EV-TR. (red=EVNW; green=EVSW; blue=EVE). See caption to Fig. 10.

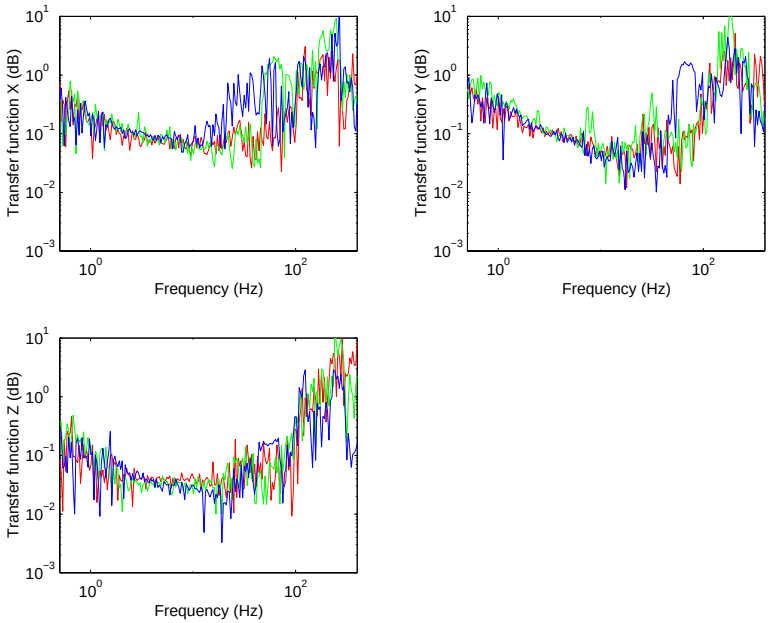

Figure 13: EE-TR. (red=EENW; green=EESW; blue=EEE). See caption to Fig. 10.

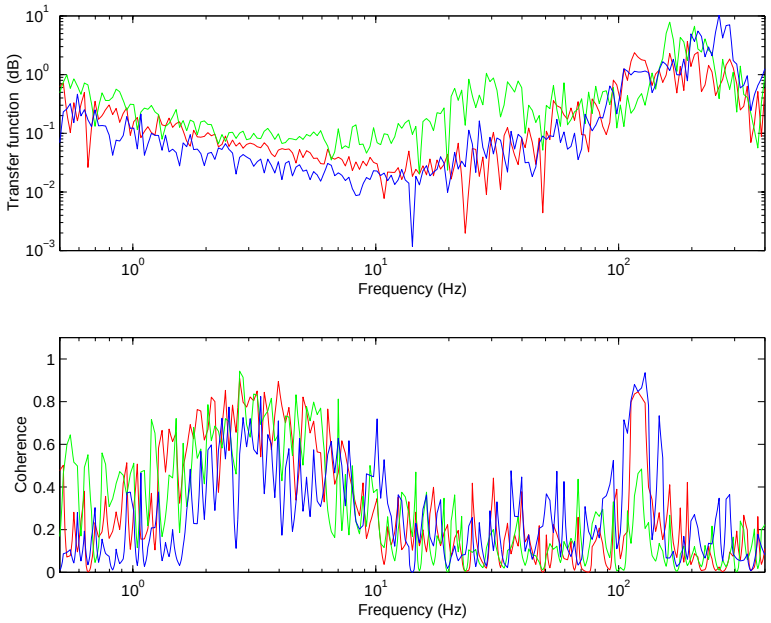

Figure 14: SE-S. Top: Transfer function between the two geophones; one on the floor, the other on the top of the bracket that rests on one of the three STACIS pedestals (in this case, the south pedestal on the south end test mass chamber). The STACIS system was turned ON. Bottom: Coherence between the two geophones. In both figures, red is x, green is y, and blue is z (vertical).

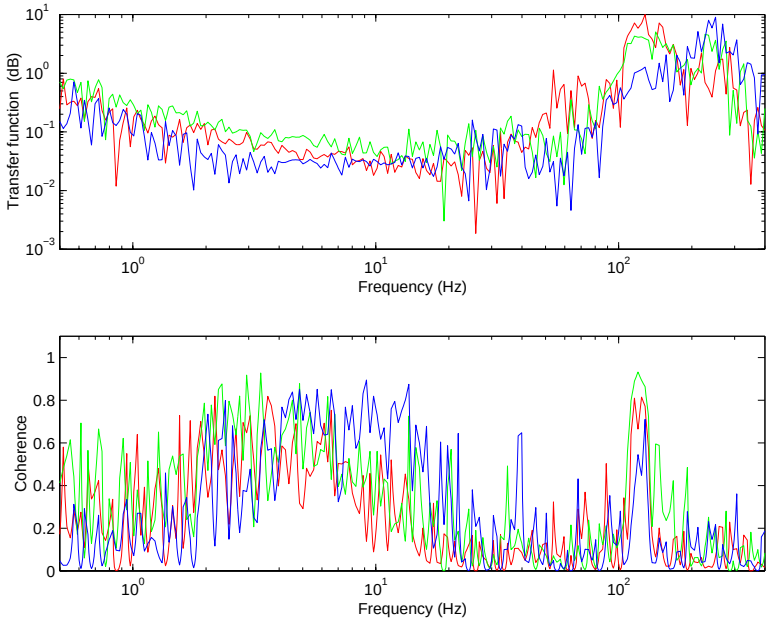

Figure 15: SE-NW. See caption to Fig. 14.

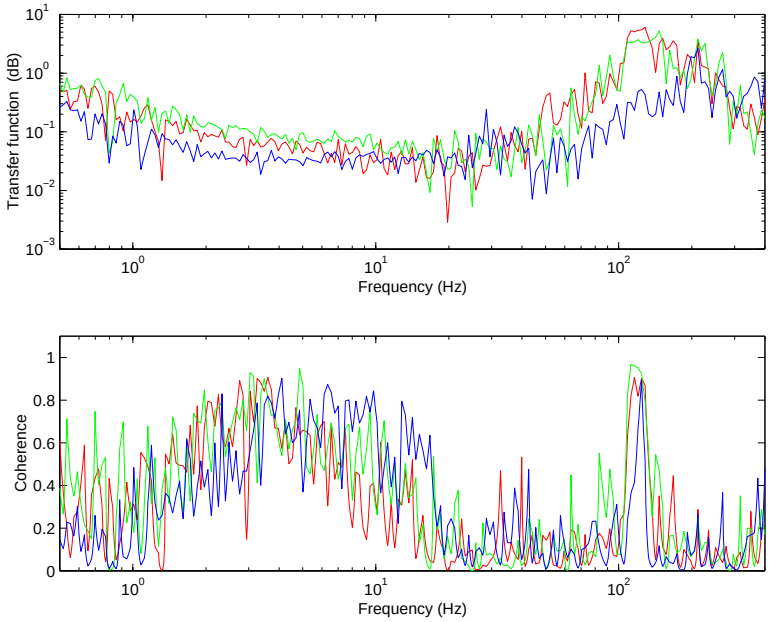

Figure 16: SE-NE. See caption to Fig. 14.

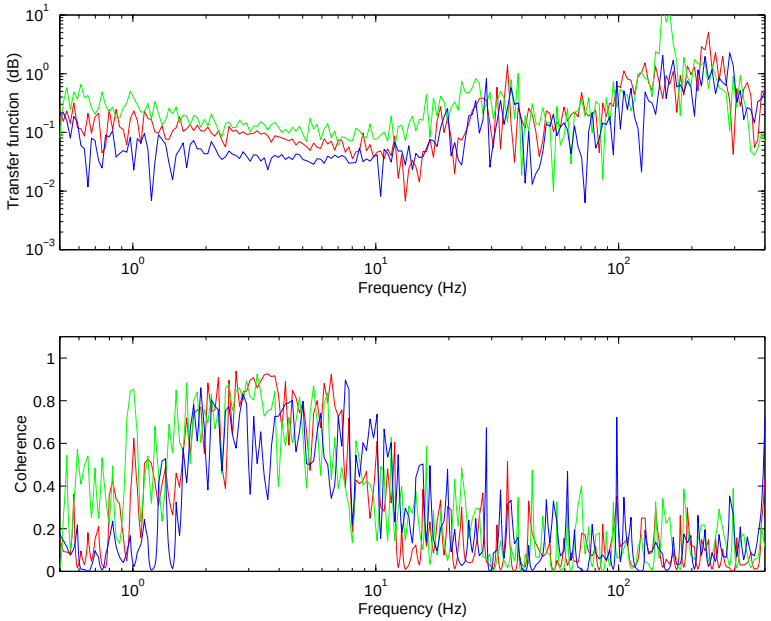

Figure 17: SV-S. See caption to Fig. 14.

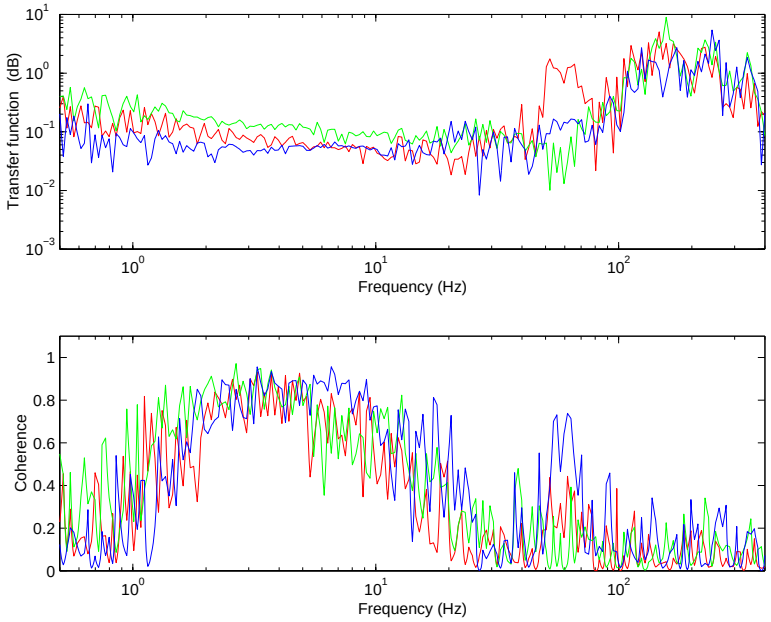

Figure 18: SV-NW. See caption to Fig. 14.

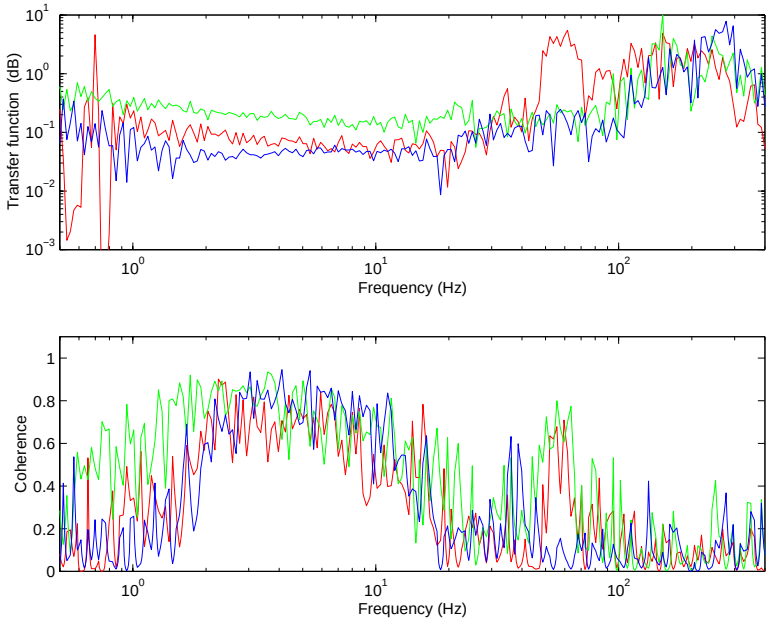

Figure 19: SV-NE. See caption to Fig. 14.

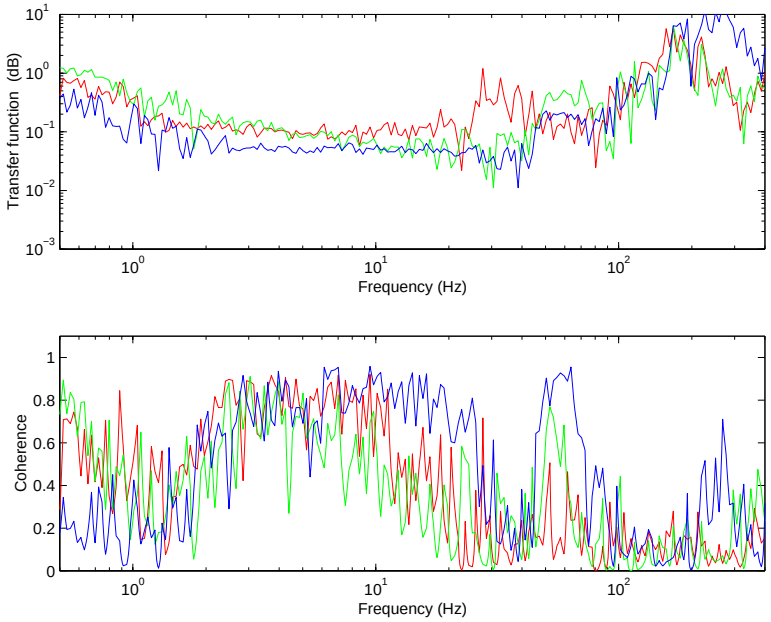

Figure 20: EV-E. See caption to Fig. 14.

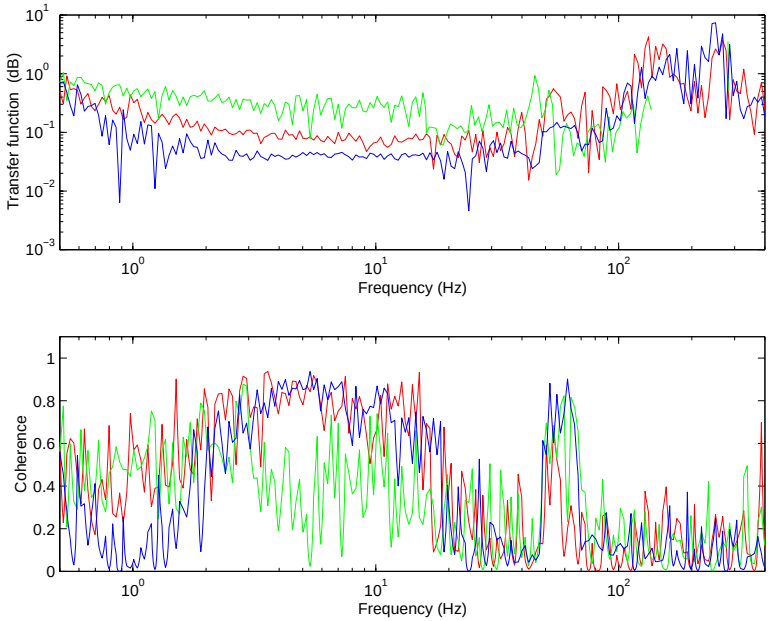

Figure 21: EV-NW. See caption to Fig. 14.

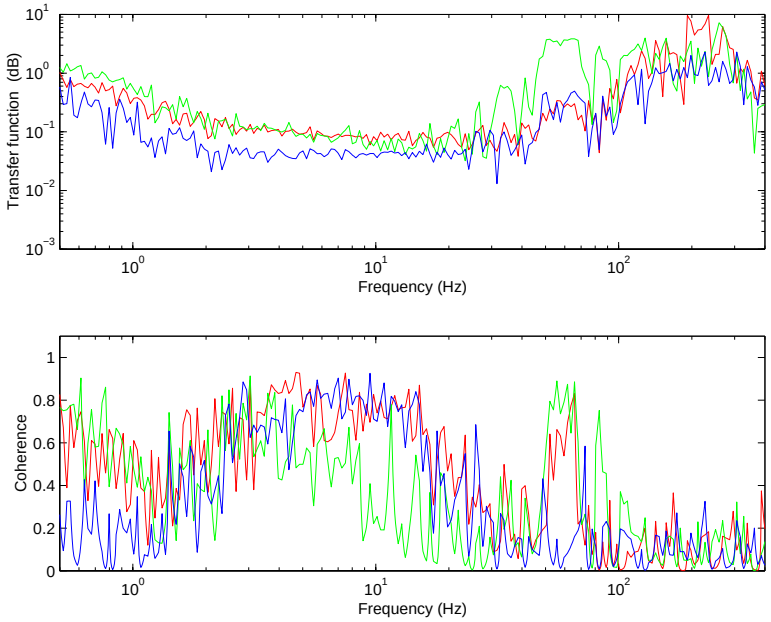

Figure 22: EV-SW. See caption to Fig. 14.

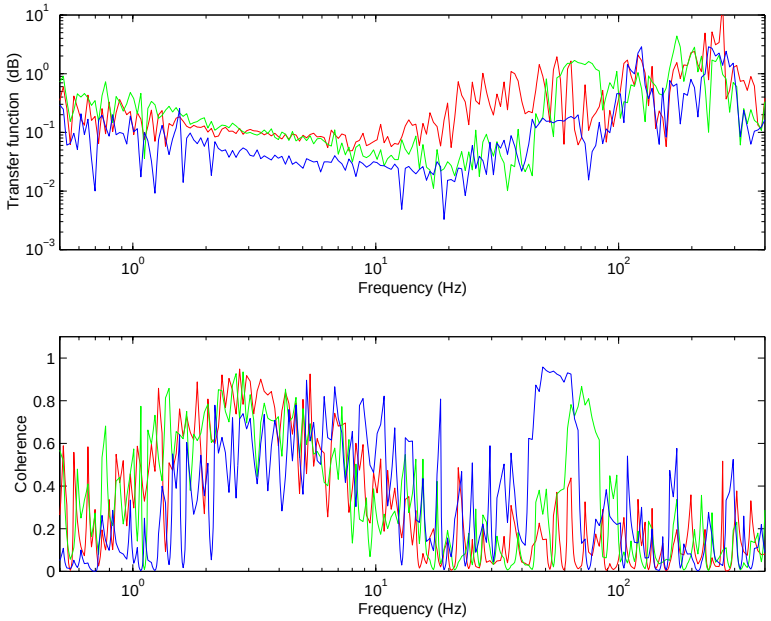

Figure 23: EE-E. See caption to Fig. 14.

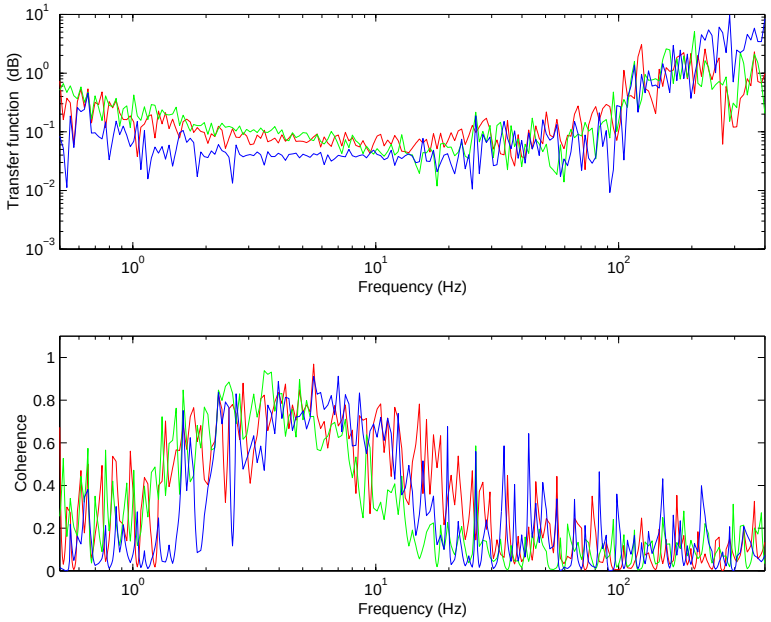

Figure 24: EE-NW. See caption to Fig. 14.

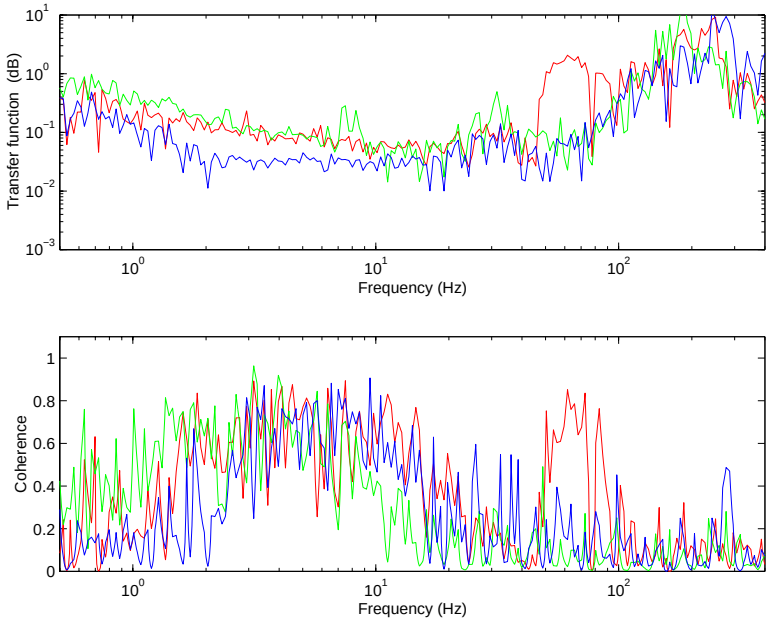

Figure 25: EE-SW. See caption to Fig. 14.

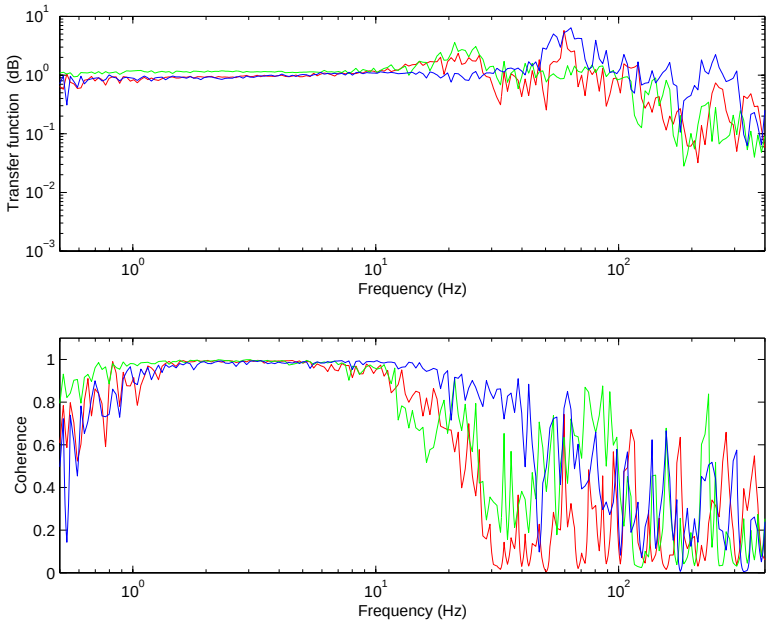

Figure 26: NOLOAD. Top: Transfer function between the two geophones; one on the floor, the other on the top of an unloaded stacis pedestal. The STACIS system was turned OFF. Bottom: Coherence between the two geophones. In both figures, red is x, green is y, and blue is z (vertical).

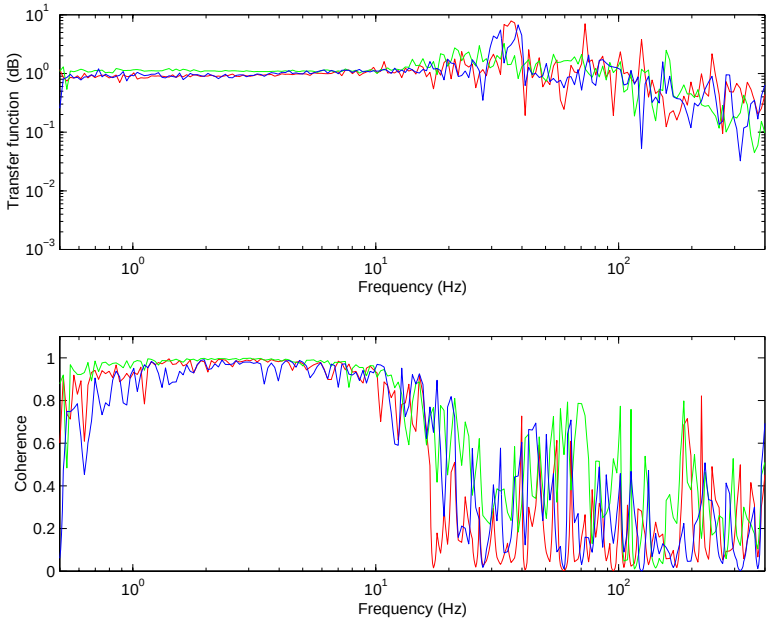

Figure 27: SVS-OFF. Top: Transfer function between the two geophones; one on the floor, the other on the top of the bracket that rests on one of the three STACIS pedestals (in this case, the south pedestal on the south vertex test mass chamber). The STACIS system was turned OFF. Bottom: Coherence between the two geophones. In both figures, red is x, green is y, and blue is z (vertical).

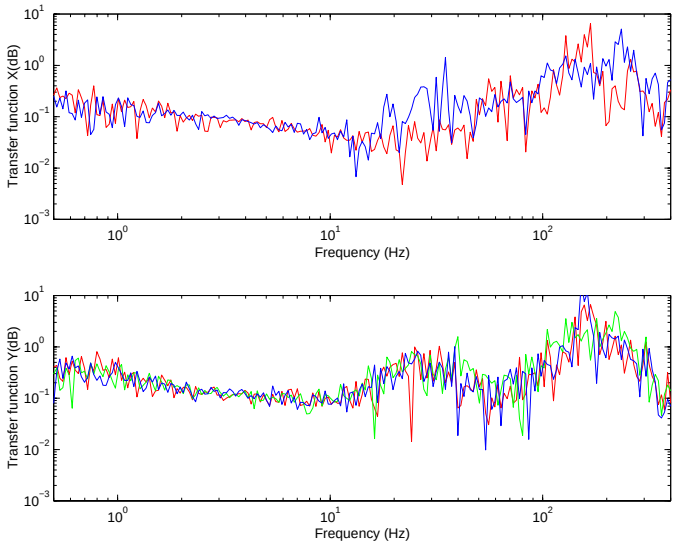

Figure 28: SVS-PLATE. Top: Transfer function between the two geophones; one on the floor, the other on the top of the bracket that rests on one of the three STACIS pedestals (in this case, the south pedestal on the south vertex test mass chamber). The STACIS system was turned ON. TOP: X; BOTTOM: Y. Blue: no plate. Green and red: alternate plate locations.

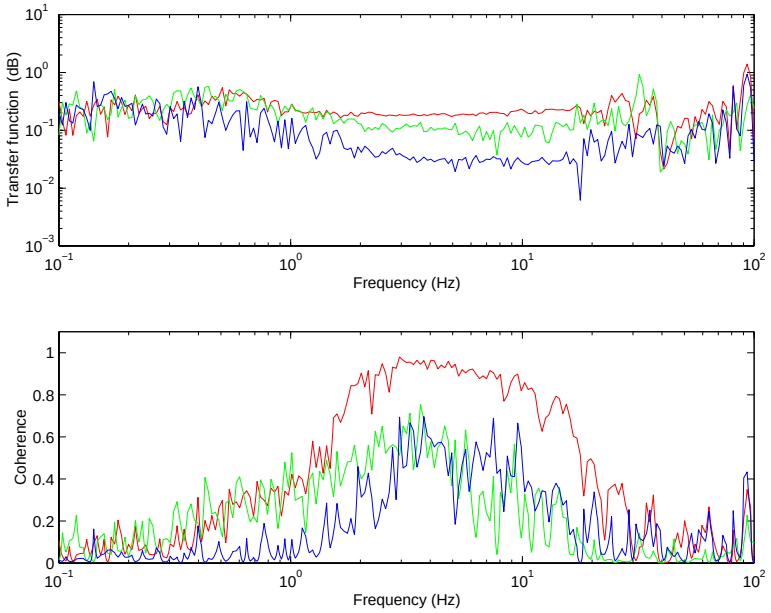

Figure 29: SES-LOW. Measurement down to 0.1 Hz. Top: Transfer function between the two geophones; one on the floor, the other on the top of the bracket that rests on one of the three STACIS pedestals (in this case, the S pedestal on the south end test mass chamber). The STACIS system was turned ON. Bottom: Coherence between the two geophones. In both figures, red is x, green is y, and blue is z (vertical).

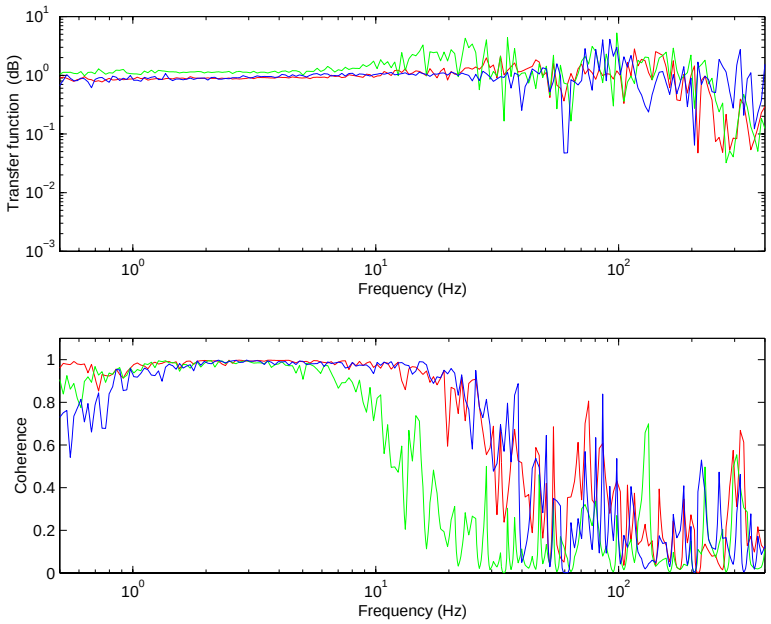

Figure 30: NOFEET. Top: Transfer function between the two geophones; one on the floor, the other on the top of the bracket that rests on one of the three STACIS pedestals (in this case, the S pedestal on the south end test mass chamber). The STACIS system was NOT YET INSTALLED (we're checking the resonances of the bracket). Bottom: Coherence between the two geophones. In both figures, red is x, green is y, and blue is z (vertical).

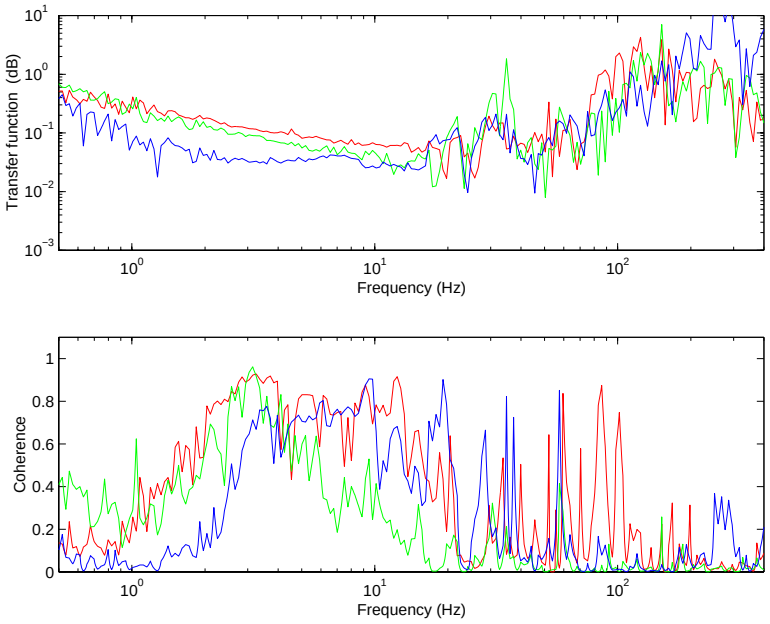

Figure 31: CLAMP. SW pedestal on the east end test mass chamber. The STACIS system was ON. The geophones were clamped to the bracket, and the number of averages increased, to see if we get better coherence at high and low frequencies, respectively. Hard to tell. Otherwise, same caption as Fig 30.

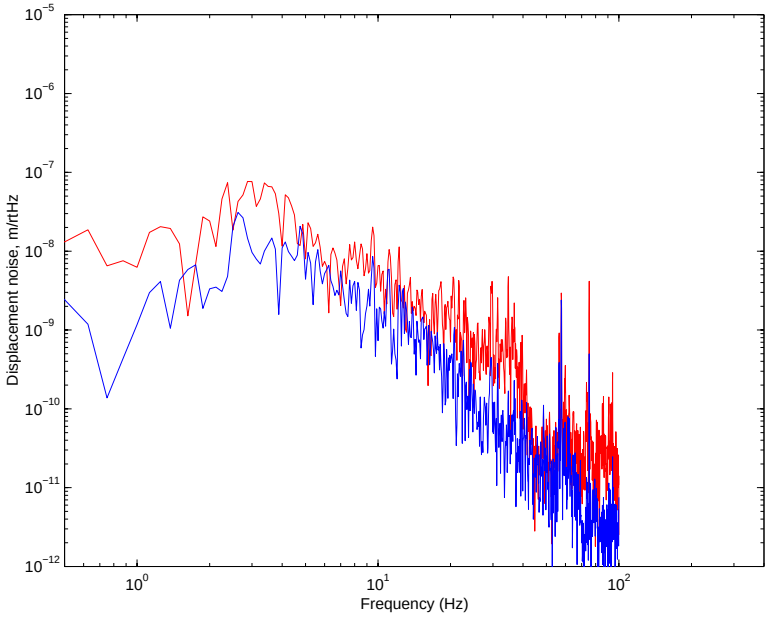

Figure 32: BRACK. Displacement noise spectrum on top of the bracket. See caveats in caption to Fig. 8. Red = horizontal, blue = vertical. We're checking the resonances of the bracket.